EVANESCENT LIQUID SOUND-PRESSURE WAVES NEAR UNDERWATER RESONATORS

Reinhart Frosch
Sommerhaldenstrasse 5B, CH-5200 Brugg, Switzerland; reinifrosch@bluewin.ch
PSI (Paul Scherrer Institute), Villigen and ETH (Eidgenoessische Technische Hochschule), Zurich (retired)

1. INTRODUCTION

Evanescent liquid sound-pressure waves (i.e., standing waves, of limited spatial extension, with variable pressure and liquid-particle velocity but negligible density variation) appear to play a fairly important role in the human cochlea, e.g., in the generation process of spontaneous oto-acoustic emissions [Frosch (2010a, 2010b)]. These waves are studied, in the present contribution, with the help of underwater resonators. Mainly because of the kinetic energy in the generated evanescent waves, a tuning fork submerged in water oscillates at a frequency below 440 Hz (typically at ~415 Hz, lower than 440 Hz by about a semitone). In the case of drinking glasses tapped with a spoon, the corresponding frequency reduction is greater than an octave; see Table 1.

Case	Condition	f [Hz]	b [Eq.(11)]
A	empty, on table	~1040	0
B	full, on table	~590	2
C	empty, submerged	~590	2
D	full, submerged	~440	4

Table 1. Frequencies of a wineglass tapped with a spoon.

In Section 2 below, an idealized drinking glass is treated, namely a bottomless hollow cylinder as shown in Fig. 1.

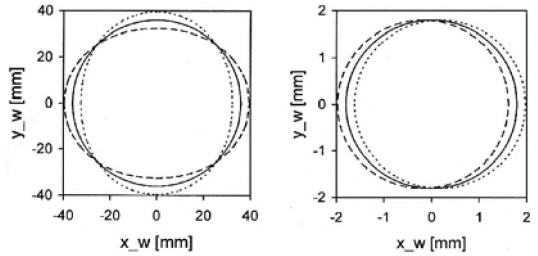

Fig. 1. Left: oscillation of idealized tapped drinking glass. Right: linear oscillation of hollow cylinder or of tuning-fork prong.

2. METHODS

The true oscillation amplitude is much smaller than that shown in Fig. 1. In the corresponding small-displacement approximation [see e.g. Frosch (2010a)] the sound-pressure p and the liquid-particle velocity v in a liquid of density ρ and of negligible compressibility and viscosity obey Newton's second law in the form

$$\rho \cdot (\partial \vec{v} / \partial t) = -\vec{\nabla} p \,, \tag{1}$$

and, in the present two-dimensional case, the Laplace equation,

$$\partial^2 p / \partial x^2 + \partial^2 p / \partial y^2 = 0 \,. \tag{2}$$

A possible (standing-wave) solution for p is:

$$p(x, y, t) = a_p(x, y) \cdot \sin(\omega \cdot t) \,, \tag{3}$$

where the angular frequency $\omega = 2\pi \cdot f$ is assumed to be constant. The real function $a_p(x, y)$ in Eq. (3) must fulfil the Laplace equation (2).

Liquid sound-pressure and streamlines: In case B (see Table 1), a solution compatible with Fig. 1 is obtained if $a_p(x, y)$ on the inside of the hollow cylinder is defined to be proportional to the real part of the analytic function $F(n_c) = n_c^{\,2}$ of the complex number $n_c = x + i \cdot y = r \cdot e^{i \cdot \varphi}$:

$$a_p = (a_{p0} / R^2) \cdot (x^2 - y^2) = a_{p0} \cdot (r / R)^2 \cdot \cos(2\varphi) \,. \tag{4}$$

In Eq. (4), R is the inner radius of the hollow cylinder, a_{p0} is a pressure constant, and r, φ are plane polar coordinates. In Fig. 2 (diagram on the left), lines of constant a_p are shown to be hyperbolae.

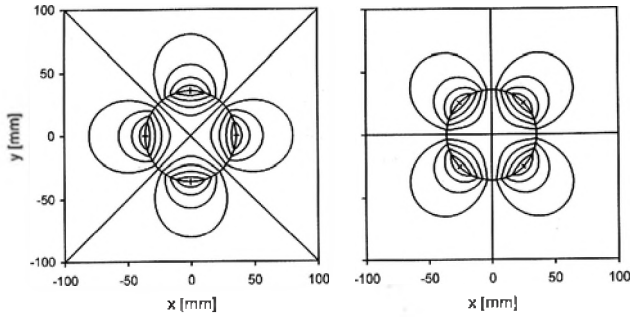

Fig. 2. Left: constant-pressure lines, $a_p / a_{p0} = 0.0, \pm 0.2, \ldots, \pm 1.0$, according to Eqs. (4) and (9). Right: streamlines according to Eqs. (6) and (10), for $N = 5$.

Eqs. (1), (3), (4) and the definitions $v_x = \partial \xi / \partial t$, $v_y = \partial \eta / \partial t$ yield the following equations for the displacements of the liquid particles from their no-wave place x, y:

$$\xi = \frac{2a_{p0} \cdot x}{\omega^2 \cdot \rho \cdot R^2} \cdot \sin(\omega t); \; \eta = -\frac{2a_{p0} \cdot y}{\omega^2 \cdot \rho \cdot R^2} \cdot \sin(\omega t) \,. \tag{5}$$

The *streamlines* of this liquid motion can be found by setting the *imaginary part* of the above-mentioned function $F(n_c) = n_c^{\,2}$ equal to a constant. The equation of streamline number n, where $n = 1, 2, \ldots, N$, is:

$$y = \pm n \cdot R^2 / (2N \cdot x) \,. \tag{6}$$

These streamlines are hyperbolae, too; see Fig. 2 (diagram on the right). A liquid particle touching the wall [no-wave coordinates $x = R \cdot \cos(\varphi)$, $y = R \cdot \sin(\varphi)$] has, according to Eq. (5), the following with-wave coordinates x_w, y_w:

$$x_w = R \cdot \cos(\varphi) \cdot [1 + \varepsilon \cdot \sin(\omega t)]; \; \varepsilon \equiv 2a_{p0} / (\omega^2 \cdot \rho \cdot R^2) \,; \tag{7}$$

$$y_w = R \cdot \sin(\varphi) \cdot [1 - \varepsilon \cdot \sin(\omega t)] . \quad (8)$$

The contours in the x_w-y_w plane defined by Eqs. (7) and (8) at $\omega t = 0, \pi/2, \pi,$ and $3\pi/2$ agree with the hollow-cylinder shapes shown in Fig. 1 (left).

In case C (Table 1), derivations like those just described, but based on the function $F(n_c) = n_c^{-2}$ of the number $n_c = x + i \cdot y = r \cdot e^{i \cdot \varphi}$, yield the following equations:

$$a_p = a_{p0}' \cdot (R'/r)^2 \cdot \cos(2\varphi); \; R' = \text{outer cylinder radius} ; \quad (9)$$

$$\text{streamlines: } r(\varphi) = R' \cdot \sqrt{(N/n) \cdot \sin(2\varphi)} ; \quad (10)$$

see Fig. 2 (regions outside of cylinder).

Prediction of oscillation frequencies: If the potential energy during the oscillation shown in Fig. 1 (left) is assumed to be due to the deviation of the local curvature radii of the half-thickness line from the no-wave radius $R_{av} = (R + R')/2$, then the following theoretical oscillation frequency is obtained [Frosch (2010a)]:

$$f_{th} = [h/(\pi \cdot R_{av}^2)] \cdot \sqrt{(Y \cdot h)/(5h \cdot \rho_w + b \cdot R_{av} \cdot \rho)} ; \quad (11)$$

here, $h = R' - R$ = wall thickness, assumed to be $<< R_{av}$; Y = elasticity modulus of wall; ρ_w = density of wall; b = number depending on the considered case (see Table 1).

Oscillation of hollow cylinder according to Fig. 1 (right): In that case, the functions $F(n_c) = n_c$ and $F(n_c) = n_c^{-1}$ yield straight equidistant lines on the inside and circles on the outside of the hollow cylinder; see Fig. 3 and Eqs (12),(13).

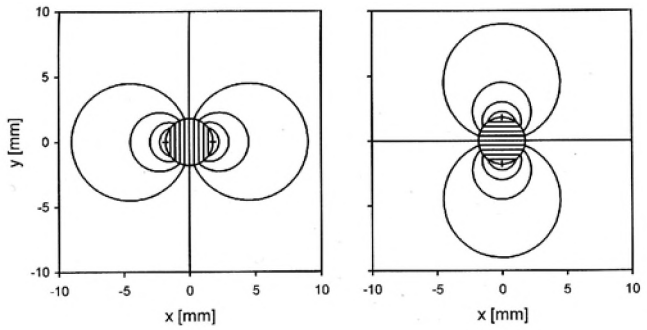

Fig. 3. As Fig. 2, but for hollow-cylinder oscillation as shown in Fig. 1 (right).

Liquid-pressure amplitude (Fig. 3, left):

$$r < R : a_p = a_{p0} \cdot x/R; r > R' : a_p = a_{p0}' \cdot (R'/r) \cdot \cos(\varphi) . \quad (12)$$

Streamlines (Fig. 3, right):

$$r < R : y = \pm R \cdot n/N; r > R' : r = R' \cdot (N/n) \cdot \sin(\varphi) . \quad (13)$$

The hollow cylinder and all liquid particles inside oscillate together in the x-direction.

The oscillation of an idealized tuning-fork prong is also illustrated by Fig. 1 (right) and Fig. 3. During a sinusoidal oscillation of frequency $f = \omega/(2\pi)$ and amplitude $\varepsilon' \cdot R'$, the maximal kinetic energies of the prong (radius R', height H, density ρ_{prong}) and of the surrounding water are [Frosch (2010a)]:

$$E_{prong} = (\pi/2) \cdot R'^4 \cdot H \cdot \rho_{prong} \cdot \varepsilon'^2 \cdot \omega^2 ; \quad (14)$$

$$E_{water} = (\pi/2) \cdot R'^4 \cdot H \cdot \rho \cdot \varepsilon'^2 \cdot \omega^2 . \quad (15)$$

Eqs. (14),(15) yield the following prediction for the tuning-fork frequency ratio $R_f = f(\text{in air})/f(\text{under water})$:

$$R_f = \sqrt{1 + \rho/\rho_{prong}} . \quad (16)$$

3. RESULTS

Insertion of the properties of the wineglass used for Table 1 into Eq. (11) yielded, for case A (i.e., $b = 0$), a prediction of $f_{th} = (0.70 \pm 0.10)$ kHz, lower than the experimental frequency of 1.04 kHz; such a discrepancy is expected, because the glass structure differs strongly from the assumed hollow cylinder (Fig. 1). Eq. (11) correctly predicts equal frequencies in cases B and C. Various hollow metal cylinders yielded good agreement of theory with experiment in case A [Frosch (2010a)]. A typical experimental D/A frequency reduction factor was (0.52 ± 0.01), larger than the factor of (0.42 ± 0.01) predicted by Eq. (11). That discrepancy is attributed to the small height H of the cylinder used $(H/R_{av} = 1.03)$; true streamlines agreed with Fig. 2 near half-height only. Insertion of the steel density $\rho_{prong} = 8.0\,\text{g/cm}^3$ into Eq. (16) yields a predicted frequency ratio of $R_f = 1.061$, corresponding to one semitone, in agreement with observation.

4. CONCLUSION

The experimentally observed oscillation frequency reductions caused by submerging resonators in water are consistent with the hypothesis that these reductions are predominantly due to the kinetic energy of the evanescent (standing) waves generated by the resonators.

REFERENCES

Frosch, R. (2010a). Introduction to Cochlear Waves. vdf, Zurich, pp. 257-279, 301-302, 423-426.

Frosch, R. (2010b). Analysis of Human Oto-Acoustic Emissions. Contribution to this conference.